J. Fluid Mech. (1992), *vol.* 236, *pp.* 167–196
Printed in Great Britain

Non-isothermal flow of a liquid film on a horizontal cylinder

By B. REISFELD† AND S. G. BANKOFF
Department of Chemical Engineering, Northwestern University, Evanston, IL 60208, USA

(Received 6 August 1990 and in revised form 5 August 1991)

We consider the flow of a viscous liquid film on the surface of a cylinder that is heated or cooled. Lubrication theory is used to study a thin film under the influence of gravity, capillary, thermocapillary, and intermolecular forces. We derive evolution equations for the interface shapes as a function of the azimuthal angle about the cylinder that govern the behaviour of the film subject to the above coupled forces. We use both analytical and numerical techniques to elucidate the dynamics and steady states of the thin layer over a wide range of thermal conditions and material properties. Finally, we extend our derivation to the case of three-dimensional dynamics and explore the stability of the film to small axial disturbances.

1. Introduction

The flow and stability of thin, free-surface films are of importance to many processes arising in the fields of chemical and mechanical engineering. Non-isothermal films, in particular, because of their importance in coating and heat transfer applications, have been the source of both experimental and theoretical investigations for a number of years.

The flow of heated thin films on inclined surfaces has been the subject of a number of studies over the past two decades. Bankoff (1971) studied the flow and stability of an evaporating liquid film draining down an inclined heated plate, assuming that the evaporating interface is always maintained at the saturation temperature. Lin (1975) extended this work to account for variations in the interfacial temperature and included the effects of variable surface tension. Spindler (1982) later considered the full linear stability problem, taking into account the development in the mean thickness of the film owing to evaporation as it drains down the wall, and also included the induced vapour shear stress.

There have been relatively few studies in the stability of heated volatile or non-volatile films on horizontal substrates. Davis (1983) examined the behaviour of a non-volatile film on a uniformly-heated horizontal substrate. He derived the evolution equation describing the layer thickness, taking into account surface tension, thermocapillary forces, and van der Waals attractions. This analysis was extended to volatile layers by Burelbach, Bankoff & Davis (1988) who, in addition to those effects listed above, also included fluid evaporation and vapour recoil. They examined in detail the linear and nonlinear stability of the thin film, especially as they related to film rupture and dryout. The dynamics and steady-states of films on

† Present address: Department of Biomedical Engineering, The Johns Hopkins School of Medicine, Baltimore, MD 21205, USA.

horizontal substrates with spatial temperature variations were later examined theoretically by Tan, Bankoff & Davis (1990), and experimentally by Burelbach, Bankoff & Davis (1990).

Another aspect of interfacial flows concerns threads or annuli of fluid. Rayleigh (1879) discussed the instability of a cylinder of inviscid liquid and found that $2\pi R/\lambda = 0.696$ for the most rapidly growing mode, where R is the radius of the jet and λ is the disturbance wavelength. Goren (1962) examined the instability of an *isothermal* annular coating of liquid on a wire, and found, when the film is very thin, that the most rapidly growing disturbance had a wavelength satisfying $2\pi R/\lambda = 0.707$. Xu & Davis (1985) showed when axial temperature gradients are present and thermocapillarity induces axial flow that the capillary breakup of jets can be retarded or suppressed entirely, depending on the magnitude of the Prandtl and Biot numbers.

Here we consider the flow of a thin liquid film on the surface of a heated or cooled horizontal cylinder. This type of flow is important in a number of applications, including the extrusion of pipe or wire coatings, fluid flow over cylindrical packing material in chemical beds, and film flow over tubes in heat-transfer devices.

As in the former cases, gravity, surface tension, thermocapillarity and, in the case of very thin films, van der Waals interactions can all be important. However, this flow is quite different from that along an inclined or a horizontal substrate, primarily because the effect of gravity on the flow depends upon the position (azimuthal angle) about the substrate. This spatially varying body force is also important in the coating flow on or inside a rotating horizontal cylinder, examined in detail by Moffatt (1977), Preziosi & Joseph (1988), and Johnson (1988).

For film flow on the surface of a stationary horizontal cylinder the primary manifestation of this configuration is that an initially uniform unperturbed interface instantly becomes position dependent as the fluid begins to drain. Moreover, when intermolecular forces are present, the position-dependent body force can lead eventually to film rupture at a single point (as in the horizontal case) or at two points, depending on the magnitude of surface tension and gravity.

In general, the flow properties and dynamics of the free surface of the film are influenced to a great extent by the thermal conditions at the surface of the cylinder as well as those at the liquid/gas interface. For an isothermal film, the liquid drains off the exterior of the substrate under the influence of gravitational forces, restrained only by surface tension and the viscous stress exerted by the substrate surface. An important parameter governing the film flow properties is the Bond number, a measure of the ratio of gravitational to surface tension forces; at large Bond number, the film will eventually flow completely off the surface. If the Bond number is small enough, however, the film can assume a steady-state shape about the axis of the cylinder.

For a heated or cooled cylinder, the Biot number characterizes the type of heat transfer that occurs at the free surface. Very large Biot numbers indicate a free-surface equilibrium for the film, while very small Biot numbers denote an adiabatic film. For the non-isothermal film, interfacial temperature variations are possible and these may lead to surface-tension-driven flows, the magnitude of which are determined by a Marangoni number. For a fluid on a heated cylinder, thermocapillary forces augment the effect of gravity and increase the rate of drainage from the substrate. If the cylinder is cooled, thermocapillary effects oppose drainage from the surface and it is possible to restrain the layer for even large Bond number.

We explore the role of gravity, surface tension, thermocapillarity, and inter-

molecular forces on a non-isothermal film draining off the surface of horizontal cylindrical substrate. We study the possibility of steady states for the film under a variety of thermal conditions, and also investigate the early-time dynamics of the film. We examine the role of surface tension and gravity in determining the azimuthal location of local thinning for the film and investigate the influence of intermolecular forces in promoting rupture of these thin regions.

We develop a two-dimensional evolution equation accounting for both azimuthal and axial variations to the film thickness, and using linear theory, we analyse the stability of the film to determine the effect of axial perturbations to the basic state of the thin layer.

2. Formulation

We consider a thin liquid film on a horizontal cylinder. In this work, we restrict our attention to two-dimensional flows with no axial variations. We shall investigate this restriction and its implications in §8 of this work. As shown in figure 1, we use a polar coordinate system with the cylinder centre located at $r = 0$ and the azimuthal angle θ measured downward from vertical. The surface of the cylinder is located at $r = R$ and is kept at a constant temperature $T = T_0$. The film consists of a non-volatile Newtonian liquid with constant material properties, bounded by a passive gas whose viscosity and thermal conductivity are assumed to be very small compared to those of the liquid; the far-field gas temperature is T_∞. For convenience, we define a new radial coordinate $\xi = r - R$, so that the substrate surface is fixed at $\xi = 0$ and the liquid/gas interface is located at $\xi = h(\theta, t)$, where t is time. The outward unit normal vector, $\boldsymbol{n}$, and unit tangent vector, $\boldsymbol{t}$, are

$$\boldsymbol{n} = (1, -h_\theta/r)/N, \quad \boldsymbol{t} = (h_\theta/r, 1)/N, \tag{2.1a, b}$$

where $N = (1 + h_\theta^2/r^2)^{\frac{1}{2}}$. We include the possibility of intermolecular forces in very thin films by augmenting the Navier–Stokes equations with an intermolecular potential function, ϕ. The resulting equations are

$$\rho(\boldsymbol{v}_t + \boldsymbol{v}\cdot\nabla\boldsymbol{v}) = -\nabla(p+\phi) + \mu\nabla^2\boldsymbol{v} - \rho\boldsymbol{g}, \tag{2.2}$$

where $\boldsymbol{v} = (u, v)$ is the velocity vector, $\boldsymbol{g} = (g\cos\theta, g\sin\theta)$ is the gravitational vector, p is the pressure in the liquid, ρ is the density and μ is the dynamic viscosity of the fluid.

We follow Ruckenstein & Jain (1974) and write the potential function as

$$\phi = \frac{A}{h^3}. \tag{2.3}$$

The dimensional Hamaker constant A' is related to A by

$$A = \frac{A'}{6\pi d_0 \nu^2}, \tag{2.4}$$

where d_0 is the initial film thickness and $\nu = \mu/\rho$ is the kinematic viscosity of the fluid. When $A' > 0$, usually called the case of negative 'disjoining pressure' (Deryagin & Kusakov 1937), intermolecular forces are destabilizing; when $A' < 0$ (Visser 1972), these forces are stabilizing.

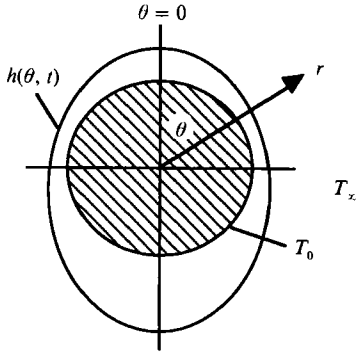

FIGURE 1. Sketch of problem geometry.

The continuity equation is

$$\nabla \cdot \boldsymbol{v} = 0. \tag{2.5}$$

An energy balance on the film yields

$$\rho C_p(T_t + \boldsymbol{v} \cdot \nabla T) = k\nabla^2 T, \tag{2.6}$$

where T is the fluid temperature, C_p is the fluid specific heat, and k is the thermal conductivity. A jump mass balance yields the kinematic condition for the interface,

$$\rho(\boldsymbol{v} - \boldsymbol{v}^{(i)}) \cdot \boldsymbol{n} = 0, \tag{2.7}$$

where $\boldsymbol{v}^{(i)}$ is the velocity of the interface. The jump in normal stress across the interface,

$$\boldsymbol{n} \cdot \boldsymbol{T} \cdot \boldsymbol{n} = 2H\sigma, \tag{2.8}$$

balances the normal stress with the product of twice the curvature and the surface tension. Here, $\boldsymbol{T} = -p\boldsymbol{I} + \tau$ is the total stress tensor, σ is the coefficient of surface tension, and $H = \frac{1}{2}\nabla \cdot \boldsymbol{n}$ is the mean curvature of the interface. The shear stress at the surface is balanced by the gradient in surface tension:

$$\boldsymbol{n} \cdot \boldsymbol{T} \cdot \boldsymbol{t} = \nabla\sigma \cdot \boldsymbol{t}, \tag{2.9}$$

where surface tension is represented by a linear equation of state

$$\sigma = \sigma_0 - \gamma(T - T_0); \tag{2.10}$$

for nearly all common liquids, $\gamma > 0$. The heat flux and the local interfacial temperature are related by

$$k\nabla T \cdot \boldsymbol{n} + h_m(T - T_\infty) = 0, \tag{2.11}$$

where h_m is the film heat transfer coefficient at the interface.

At the substrate surface there is no slip

$$u = v = 0, \tag{2.12}$$

and a constant temperature

$$T = T_0. \tag{2.13}$$

In addition, we require that h is periodic in θ, and specify symmetry conditions

$$h_\theta(0, t) = 0, \tag{2.14}$$

$$h_\theta(\pi, t) = 0, \tag{2.15}$$

and conservation of the fluid volume

$$\int_0^{2\pi} h(\theta, t)\,\mathrm{d}\theta = V_0, \tag{2.16}$$

where V_0 is the initial volume of fluid on the surface of the cylinder.

3. Scaling

The governing equations and boundary conditions are now non-dimensionalized. A characteristic lengthscale for flow in the radial (ξ) and azimuthal directions is the initial mean film thickness, d_0. Viscous scales are used for the radial and azimuthal velocities, ν/R and ν/d_0, respectively. A balance between the viscous stress and azimuthal pressure gradient leads to the pressure scale $\rho\nu^2 R/d_0^3$. A timescale for the flow is Rd_0/ν. The temperature difference, $T-T_\infty$ is scaled on its maximum difference $\Delta T = T_0 - T_\infty$.

The scaled radial component of the equations of motion is

$$\epsilon^3\left(u_t + uu_\xi + \frac{v}{1+\epsilon\xi}u_\theta - \frac{v^2}{1+\epsilon\xi}\right) = -p_\xi + \epsilon^2\left[\frac{1}{1+\epsilon\xi}[(1+\epsilon\xi)\,u]_\xi\right]_\xi + \epsilon^4\frac{1}{(1+\epsilon\xi)^2}u_{\theta\theta} - \frac{2\epsilon^3}{(1+\epsilon\xi)^2}v_\theta + 3\epsilon G\cos\theta, \tag{3.1}$$

where ϵ is the aspect ratio,

$$\epsilon = \frac{d_0}{R}, \tag{3.2}$$

and G is a gravity number which compares gravitational to viscous forces,

$$G = \frac{gd_0^3}{3\nu^2}. \tag{3.3}$$

The scaled azimuthal component takes the form

$$\epsilon\left(v_t + uv_\xi + \frac{v}{1+\epsilon\xi}v_\theta - \frac{\epsilon uv}{1+\epsilon\xi}\right) = -\frac{1}{(1+\epsilon\xi)}(p_\theta + \phi_\theta) + \left[\frac{1}{1+\epsilon\xi}[(1+\epsilon\xi)\,v]_\xi\right]_\xi + \frac{\epsilon^2}{(1+\epsilon\xi)^2}v_{\theta\theta} + \frac{2\epsilon^3}{(1+\epsilon\xi)^2}u_\theta + 3G\sin\theta. \tag{3.4}$$

The scaled community and energy equations are

$$[(1+\epsilon\xi)\,u]_\xi + v_\theta = 0, \tag{3.5}$$

and

$$\epsilon P\left(T_t + uT_\xi + \frac{v}{1+\epsilon\xi}T_\theta\right) = \frac{1}{1+\epsilon\xi}[(1+\epsilon\xi)\,T_\xi]_\xi + \frac{\epsilon^2}{(1+\epsilon\xi)^2}T_{\theta\theta}, \tag{3.6}$$

respectively, where the Prandtl number,

$$P = \frac{\rho C_p \nu}{k}, \tag{3.7}$$

relates viscous to thermal diffusion. At the liquid interface, the kinematic condition is

$$h_t + \frac{1}{1+\epsilon\xi}vh_\theta - u = 0. \tag{3.8}$$

We also have the scaled shear-stress balance

$$\frac{2\epsilon}{1+\epsilon\xi}\left(u_\xi-\frac{1}{1+\epsilon\xi}v_\theta-\frac{\epsilon u}{1+\epsilon\xi}\right)h_\theta+\left(1-\frac{\epsilon^2}{(1+\epsilon\xi)^2}h_\theta^2\right)$$
$$\left[(1+\epsilon\xi)\left(\frac{v}{1+\epsilon\xi}\right)_\xi+\frac{\epsilon^2 y_\theta}{1+\epsilon\xi}\right]=-\frac{2\epsilon M}{P}\frac{1}{1+\epsilon\xi}(T_\xi h_\theta+T_\theta)N_\epsilon, \quad (3.9)$$

where M is the Marangoni number which measures the fractional change in surface tension,

$$M=\frac{\gamma\Delta T d_0 C_p}{2k\nu}, \quad (3.10)$$

and for convenience we have defined

$$N_\epsilon=\left(1+\frac{\epsilon^2 h_\theta^2}{(1+\epsilon\xi)^2}\right)^{\frac{1}{2}}. \quad (3.11)$$

The scaled normal-stress balance is

$$p-\frac{2\epsilon^2 h_\theta}{1+\epsilon\xi}N_\epsilon^{-2}\left[\frac{\epsilon^2 h_\theta}{(1+\epsilon\xi)^2}(v_\theta+u)-(1+\epsilon\xi)\left(\frac{v}{1+\epsilon\xi}\right)_\xi+\frac{u_\theta}{1+\epsilon\xi}\right]$$
$$=-3\epsilon^3 S(1-CT)N_\epsilon^{-3}\left[\frac{N_\epsilon^2}{\epsilon(1+\epsilon\xi)}-\frac{N_\epsilon^2 h_{\theta\theta}}{(1+\epsilon\xi)^2}+\frac{\epsilon h_\theta^2}{(1+\epsilon\xi)^3}+\frac{\epsilon^2 h_\theta^2 h_{\theta\theta}}{(1+\epsilon\xi)^4}\right], \quad (3.12)$$

where S is the Weber number $$S=\frac{\sigma_0 d_0}{3\rho\nu^2}, \quad (3.13)$$

which characterizes the mean surface tension to viscous forces and C is the capillary number defined by

$$C=\frac{\gamma\Delta T}{\sigma_0}. \quad (3.14)$$

The scaled thermal flux condition is

$$T_\xi-\frac{\epsilon^2}{(1+\epsilon\xi)^2}T_\theta h_\theta+BTN_\epsilon=0, \quad (3.15)$$

where the Biot number, $$B=\frac{d_0 h_m}{k}, \quad (3.16)$$

conveys the quality of heat transfer occurring at the liquid/gas interface. In particular, $B\to 0$ and $B\to\infty$ give the adiabatic and surface-equilibrium limits, respectively.

At the surface of the cylinder, we have no slip

$$u=v=0, \quad (3.17)$$

and a constant temperature $$T=1. \quad (3.18)$$

The symmetry conditions are given by (2.14) and (2.15), and the scaled volume-conservation constraint is

$$\frac{1}{2\pi}\int_0^{2\pi}h(\theta,t)\,\mathrm{d}\theta=1. \quad (3.19)$$

	Water		Mercury	
T_0 (°C)	25		25	
ρ (g/cm^3)	1.0		13.6	
μ (g/cm s)	1.0×10^{-2}		1.6×10^{-2}	
k (erg/cm s °C)	5.8×10^{4}		8.4×10^{4}	
C_p (erg/g °C)	4.2×10^{7}		1.3×10^{6}	
σ_0 (dyne/cm)	72		475	
γ (dyne/cm °C)	0.16		0.20	
ΔT (°C)	10		10	
h_m (g/s^3 °C)	10^{5}		10^{5}	
A' (erg)	10^{-13}		10^{-13}	
g (cm/s^2)	980.6		980.6	
	Thin wire	Large tube	Thin wire	Large tube
d_0 (cm)	1×10^{-4}	0.1	1×10^{-4}	0.1
R (cm)	0.01	10	0.01	10
ϵ	0.01	0.01	0.01	0.01
C	10^{-2}	10^{-2}	10^{-3}	10^{-3}
P	10	10	10^{-2}	10^{-2}
A	10^{-6}	10^{-9}	10^{-7}	10^{-10}
S	10	10^{4}	10^{2}	10^{5}
G	10^{-6}	10^{3}	10^{-6}	10^{3}
M	10	10^{4}	10^{-2}	10
$\mathscr{R}$	10^{-2}	10	10^{-3}	1
Bo^{-1}	10	10^{-5}	10	10^{-5}
B	10^{-4}	10^{-1}	10^{-5}	10^{-2}
$\mathscr{M}$	10^{3}	10^{-3}	10^{3}	10^{-3}
$\mathscr{A}$	10^{-1}	10^{-13}	10^{-1}	10^{-13}

TABLE 1. Material properties and dimensionless groups for liquids at 1 atm

As a result of the scaling, a number of non-dimensional groups appear in the problem. Typical numerical values and the material properties from which they were computed are presented in table 1 for water and mercury, coating two different sized cylinders.

4. Lubrication theory

We consider solutions of (3.1)–(3.19) when $\epsilon \ll 1$. We assume that u, v, p, $\partial/\partial t$, $\partial/\partial\xi$, and $\partial/\partial\theta = O(1)$ as $\epsilon \to 0$, and further assume that $h(\theta, t)$ is an unspecified unit-order function. We expand the dependent variables in powers of ϵ,

$$u = u_0 + \epsilon u_1 + \epsilon^2 u_2 + O(\epsilon^3), \tag{4.1a}$$

$$w = w_0 + \epsilon w_1 + \epsilon^2 w_2 + O(\epsilon^3), \tag{4.1b}$$

$$p = p_0 + \epsilon p_1 + \epsilon^2 p_2 + O(\epsilon^3), \tag{4.1c}$$

$$\phi = \phi_0, \tag{4.1d}$$

substitute these expansions into the governing system, and equate to zero like powers of ϵ in the equations and boundary conditions, leading to a sequence of problems to solve. We then solve the leading-order system to determine the temperature, pressure, and velocity fields as a function of the film thickness. These velocities are then substituted into the kinematic boundary condition to obtain an

equation describing the evolution of the interface. This procedure is analogous to the long-wave analyses used by Benney (1966) and Atherton & Homsy (1976) for falling liquid films and those used by Williams & Davis (1982) and Burelbach *et al.* (1988) for isothermal and heated thin liquid films, respectively.

In order to retain the effects of thermocapillary forces and surface tension at leading order we require that $(M, S) = (\bar{M}\epsilon^{-1}, \bar{S}\epsilon^{-3})$, where quantities with overbars are $O(1)$ as $\epsilon \to 0$. We further require that G, P, and $B = O(1)$. Note that $C = \frac{2}{3}\epsilon^2 P^{-1}\bar{M}\bar{S}^{-1}$; thermocapillary effects do not appear at leading order in the normal-stress balance.

At leading order in ϵ, the governing system is

$$p_{0\xi} = 0, \tag{4.2}$$

$$-(p_0 + \phi_0)_\theta + v_{0\xi\xi} + 3G\sin\theta = 0, \tag{4.3}$$

$$u_{0\xi} + v_{0\theta} = 0, \tag{4.4}$$

$$T_{0\xi\xi} = 0, \tag{4.5}$$

$$\xi = h(\theta, t): \begin{cases} h_t + v_0 h_\theta - u_0 = 0, \\ v_{0\xi} = -2\bar{M}P^{-1}(T_{0\theta} + T_{0\xi} h_\theta), \\ p_0 = 3\bar{S}(\epsilon^{-1} - h - h_{\theta\theta}), \\ T_{0\xi} + BT_0 = 0, \end{cases} \tag{4.6a–d}$$

$$\xi = 0: \quad u_0 = 0, \quad v_0 = 0, \quad T_0 = 1 \tag{4.7a–c}$$

with

$$h_\theta(0, t) = 0, \tag{4.8}$$

$$h_\theta(\pi, t) = 0, \tag{4.9}$$

$$\frac{1}{2\pi}\int_0^{2\pi} h(\theta, t)\,\mathrm{d}\theta = 1. \tag{4.10}$$

The leading-order equations of motion demonstrate that the pressure is uniform through the depth of the film, and the viscous stress is balanced by the azimuthal pressure gradient and gravity. The leading-order energy equation implies that conduction is the principal mode of heat transport through the film.

We solve (4.2) subject to (4.6*c*) to find the pressure in the film

$$p_0 = p_0(\theta, t) = 3\bar{S}(\epsilon^{-1} - h - h_{\theta\theta}). \tag{4.11}$$

Equation (4.11) reveals that the pressure in the layer is equal to the surface tension times the sum of the (constant) curvature of the interface – owing to the cylindrical geometry of the substrate – and the curvature produced by the presence and deformation of the liquid surface. The temperature distribution is found by solving (4.5) subject to conditions (4.6*d*) and (4.7*c*),

$$T_0 = \frac{1 + B(h - \xi)}{1 + Bh}. \tag{4.12}$$

The temperature at the free surface is then

$$T_0(h) = \frac{1}{1 + Bh}. \tag{4.13}$$

Equation (4.13) indicates in the adiabatic limit ($B \to 0$), that the free-surface temperature $T_0(h) = 1$; in the free-surface equilibrium case ($B \to \infty$), the interfacial

temperature $T_0(h) = 0$. Substituting (4.11) into (4.3), (4.12) into (4.6*b*), and applying boundary conditions (4.6*b*) and (4.7*b*) gives the azimuthal component of velocity

$$v_0 = \tfrac{3}{2}\Phi(\xi^2 - 2h\xi) + \frac{2\bar{M}B}{P}\frac{h_\theta \xi}{(1+Bh)^2}, \tag{4.14a}$$

where

$$\Phi(\theta, t) = -[G\sin\theta + \bar{S}(h_\theta + h_{\theta\theta\theta}) + Ah^{-4}h_\theta]. \tag{4.14b}$$

Combining the continuity and kinematic conditions, we arrive at an alternative form for the conservation of mass condition,

$$h_t + \left[\int_0^h v_0(\xi, t)\,\mathrm{d}\xi\right]_\theta = 0. \tag{4.15}$$

Substituting (4.14) into (4.15) we obtain

$$h_t + \left\{h^3[G\sin\theta + \bar{S}(h_\theta + h_{\theta\theta\theta})] + \frac{B\bar{M}}{P}\frac{h^2 h_\theta}{(1+Bh)^2} + Ah^{-1}h_\theta\right\}_\theta = 0. \tag{4.16}$$

The gravity number can be removed from (4.16) by rescaling the time variable as $\tau = Gt$, leading to

$$h_\tau + \left\{h^3[\sin\theta + Bo^{-1}(h_\theta + h_{\theta\theta\theta})] + B\mathscr{M}\frac{h^2 h_\theta}{(1+Bh)^2} + \mathscr{A}h^{-1}h_\theta\right\}_\theta = 0, \tag{4.17}$$

where $\mathscr{M} = \bar{M}/PG$ and $\mathscr{A} = A/G$ are an effective Marangoni number and Hamaker constant, respectively, and Bo is the Bond number defined by

$$Bo = \frac{\rho g R^3}{d_0 \sigma_0}, \tag{4.18}$$

which relates the gravity forces to mean surface tension.

Equation (4.17) describes the free-surface evolution of a thin liquid film on the surface of a heated or cooled horizontal cylinder when gravity, capillary, thermocapillary, and intermolecular forces are appreciable. This evolution equation, with appropriate boundary and initial conditions, obviates the need to solve the free-boundary problem specified by (2.1)–(2.16).

Although (4.17) is a strongly nonlinear partial differential equation, it may be solved analytically for the steady-state and dynamic interfacial behaviour in certain specific limits of interest. In general, however, we must solve the evolution equation numerically as part of an initial-boundary-value problem with periodic boundary conditions and the constant-thickness initial condition

$$h(\theta, 0) = 1. \tag{4.19}$$

The numerical solution is realized using a Fourier spectral method with 64 spectral modes and time-marching accomplished using a fourth-order Hamming modified predictor–corrector method.

5. Results – isothermal film

Having derived a general equation for a heated or cooled cylinder, it is of interest first to examine an isothermal film (for which $\mathscr{M} = 0$). In this case, the appropriate evolution equation is

$$h_\tau + \{h^3[\sin\theta + Bo^{-1}(h_\theta + h_{\theta\theta\theta})] + \mathscr{A}h^{-1}h_\theta\}_\theta = 0, \tag{5.1}$$

with symmetry boundary conditions (4.8)–(4.9) and the mass-conservation constraint (4.10).

5.1. *Steady states*

5.1.1. *Unit-order Bond number*, $\mathscr{A} = 0$

In the absence of can der Waals forces, the steady-state form of (5.1) is

$$\{h^3[\sin\theta + Bo^{-1}(h_\theta + h_{\theta\theta\theta})]\}_\theta = 0, \tag{5.2}$$

which is a balance between gravity and surface tension. Integrating (5.2) and applying symmetry conditions, we obtain an equation analogous to that for a harmonic oscillator forced at resonance, namely

$$h_{\theta\theta} + h = \vartheta + Bo\cos\theta, \tag{5.3}$$

where ϑ is an arbitrary constant. There is no 2π-periodic film thickness satisfying (5.3), except when the Bond number is vanishingly small. In this case the solution is $h(\theta) \equiv 1$; gravitational forces are negligible compared to the force of surface tension and the film maintains its initial configuration. Steady states are physically possible for films with $Bo > 0$, for instance in the case of pendant drops (Pitts 1973), but these are not well described by (5.3) because of the lubrication approximation used in its derivation.

5.1.2. *Large Bond number*, $\mathscr{A} < 0$

When the Bond number is large and destabilizing van der Waals forces are present, no steady state for the film is possible since, as the film begins to drain, surface tension is insufficient to restrain the flow; moreover, the intermolecular forces enhance the fluid drainage, producing a 'squeeze' pressure which acts to thin regions of the film which are thinner than surrounding regions.

Roughly speaking, if the dielectric constant of the solid substrate is greater than that of the liquid layer, then $A' < 0$ (Lifshitz 1956) and van der Waals forces are stabilizing. In this case, a steady-state balance can be written between fluid drainage and intermolecular forces plus surface tension:

$$\{h^3[\sin\theta + Bo^{-1}(h_\theta + h_{\theta\theta\theta})] - \mathscr{A}h^{-1}h_\theta\}_\theta = 0, \tag{5.4}$$

where $\mathscr{A} = |\mathscr{A}|$. The solution of (5.4) for large Bond numbers, subject to symmetry conditions is

$$h \sim \left(\alpha_1 + \frac{3}{\mathscr{A}}\cos\theta\right)^{-\frac{1}{3}} + Bo^{-1}\left(\alpha_1 + \frac{3}{\mathscr{A}}\cos\theta\right)^{-\frac{4}{3}}\left[\frac{4}{\mathscr{A}^3}\left(\alpha_1 + \frac{3}{\mathscr{A}}\cos\theta\right)^{-\frac{7}{3}}\sin^2\theta\right.$$
$$\left. + \frac{1}{\mathscr{A}^2}\left(\alpha_1 + \frac{3}{\mathscr{A}}\cos\theta\right)^{-\frac{4}{3}}\cos\theta + \frac{1}{\mathscr{A}}\left(\alpha_1 + \frac{3}{\mathscr{A}}\cos\theta\right)^{-\frac{1}{3}} + \alpha_2\right], \tag{5.5}$$

where α_1 and α_2 are determined from the volume-conservation condition (3.19). As depicted in figure 2, as the effective Hamaker constant is increased, the film interface is deformed less and less from the initial shape, as intermolecular forces increasingly counter the deformation due to gravity. The interface retains its initial conformation for large $\mathscr{A}$ as the gravity-driven flow downward is inhibited completely.

In figure 2 and all figures depicting the film on the substrate surface, we have exaggerated the film thickness relative to the cylinder radius to better illustrate the free-surface configuration and dynamics; the actual film thickness is 2ϵ times that pictured. The evolution equation and all subsequent results were derived on the basis of lubrication theory and a small aspect ratio for the film; all results should be interpreted in this light.

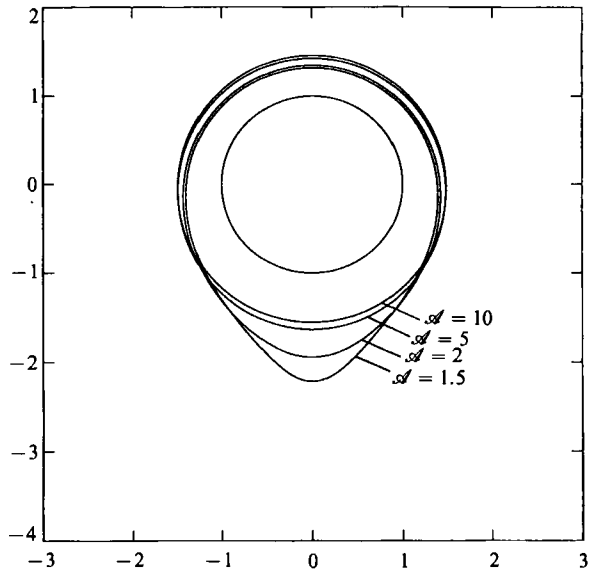

FIGURE 2. Steady-state profiles for the isothermal film when stabilizing van der Waals forces are appreciable. (The actual film thickness is 2ϵ times that shown.)

5.2. *Unsteady flow*

When a steady-state configuration is not possible, or when the film is evolving towards a steady-state shape, the dynamics are governed by (5.1).

5.2.1. *Small Bond number – early-time dynamics*

When the Bond number is small and van der Waals forces are negligible, perturbation theory may be used to find the solution of (5.1) at early times. Defining a 'fast' timescale $\tilde{t} = Bo^{-1}\tau = \bar{S}t$, we find the following solution for the layer thickness:

$$h \sim 1 - Bo\,\tilde{t}\cos\theta + \tfrac{1}{48}Bo^2(-1 + \mathrm{e}^{-12\tilde{t}} + 12\tilde{t})\cos(2\theta). \tag{5.6}$$

This solution breaks down as $\tilde{t} \to 1/Bo$ as the higher-order terms become comparable to those of leading order. Figure 3 illustrates the film dynamics at early times. As time increases, the film deforms into an ellipse about the axis of the cylinder, but interestingly, the film thickness [to $O(Bo)$] always remains at its initial value at the equator of the cylinder ($\theta = \frac{1}{2}\pi, -\frac{1}{2}\pi$), regardless of the time.

The presence of the $O(Bo^2)$ term reveals the possibility of local extrema in the film thickness in addition to those represented in the lower-order terms. The azimuthal location of these extrema (which are local minima) is

$$\theta_{\mathrm{m}} = \cos^{-1}\left[\frac{12\tilde{t}Bo^{-1}}{-1 + \mathrm{e}^{-12\tilde{t}} + 12\tilde{t}}\right]. \tag{5.7}$$

5.2.2. *Very large Bond number, $\mathscr{A} = 0$*

In the limit of very large Bond number ($Bo^{-1} \to 0$) and negligible van der Waals forces, (5.1) may be written as

$$h_\tau + (h^3 \sin\theta)_\theta = 0. \tag{5.8}$$

The solution of this equation can be obtained in implicit form via the method of characteristics. We consider the curve

$$\mathrm{d}\theta/\mathrm{d}\tau = 3h[\theta(\tau), \tau]^2 \sin\theta. \tag{5.9}$$

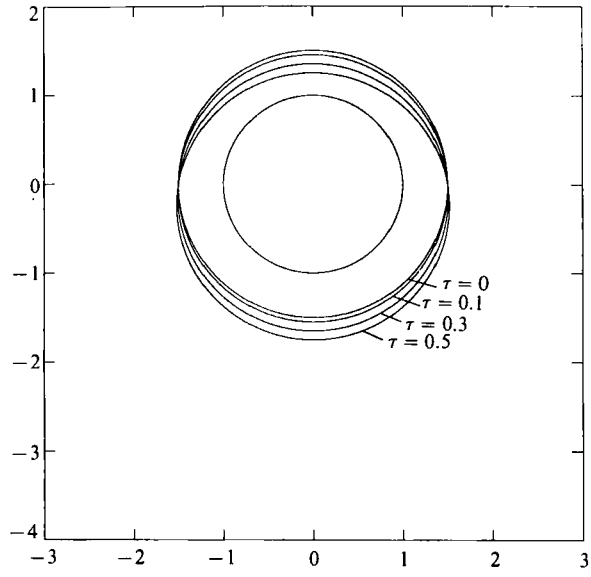

FIGURE 3. Early-time dynamics for the isothermal film when the Bond number is small and van der Waals forces are absent. (The actual film thickness is 2ϵ times that shown.)

Upon this curve (5.8) reduces to the ordinary differential equation

$$\mathrm{d}h/\mathrm{d}\tau = -h^3\cos\theta. \tag{5.10}$$

Equations (5.9) and (5.10) are solved subject to $\theta(0) = \theta_0$ and $h(\theta, 0) = 1$, which leads to the following implicit form of the solution:

$$h(\theta,\tau) = \begin{cases} \dfrac{1}{(1+2\tau)^{\frac{1}{2}}} & (\theta = \theta_0 = 0) \\ \dfrac{1}{(1-2\tau)^{\frac{1}{2}}} & (\theta = \theta_0 = \pi) \\ \left(\dfrac{\sin\theta_0}{\sin\theta}\right)^{\frac{1}{3}} & (0 < \theta < 2\pi, \theta \neq \pi). \end{cases} \tag{5.11a}$$

The time dependence of the azimuthal angle is given implicitly as the solution of

$$F[g(\theta), \sin 75°] - F[g(\theta_0), \sin 75°] + 2(3)^{\frac{1}{4}}(\sin\theta_0)^{\frac{2}{3}}\tau = 0, \tag{5.11b}$$

where

$$F[\phi, k] = \int_0^{\phi} \frac{\mathrm{d}\alpha}{(1-k^2\sin^2\alpha)^{\frac{1}{2}}} \tag{5.11c}$$

is the incomplete elliptic integral of the first kind whose first argument is

$$g(\xi) = \arccos\left(\frac{3^{\frac{1}{2}} - 1 + \sin\xi^{\frac{2}{3}}}{3^{\frac{1}{2}} + 1 - \sin\xi^{\frac{2}{3}}}\right). \tag{5.11d}$$

As shown in figure 4, (5.11) point out for a film with very large Bond number, that fluid flows from the upper hemicylinder towards a cusp point on the bottom of the cylinder, causing a localized thinning near $\theta = 0$. At larger times, the fluid drains off the cylinder in a thin filament at a position $\theta = \pi$. We observe that (5.11) predicts

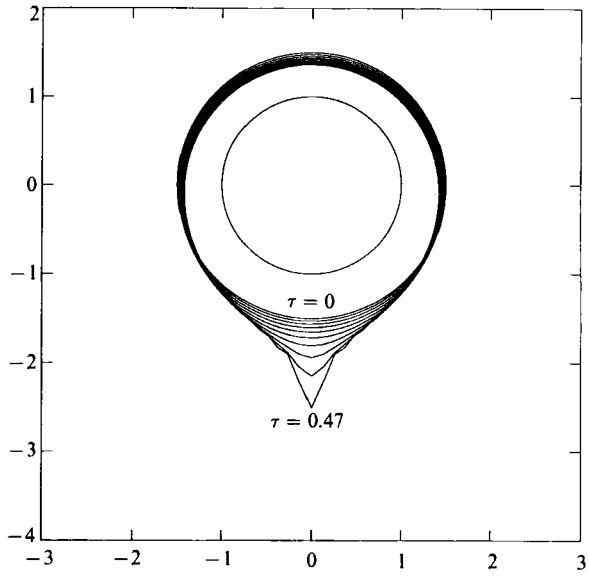

FIGURE 4. Unsteady film flow for the isothermal film with $Bo^{-1} = 0, \mathscr{A} = 0$. (The actual film thickness is 2ϵ times that shown.)

that the film profile will become singular at $\theta = \theta_0 = \pi$ as $\tau \to \frac{1}{2}$; however, because of our lubrication approximation, these equations are appropriate only at earlier times (approximately up to $\tau = 0.47$).

The cusp predicted by (5.11) arises because the highest spatial derivative term in (5.1) is omitted with $Bo^{-1} = 0$, and a boundary layer hence develops at $\theta = \pi$. This boundary-layer structure may be resolved using singular perturbation theory. Introducing a boundary-layer coordinate $\zeta = (\theta - \pi)/\Delta$ into (5.1) (with $\mathscr{A} = 0$), we find for very large Bo that the boundary-layer thickness Δ is

$$\Delta = O(Bo^{-\frac{1}{4}}). \tag{5.12}$$

This thickness gives an indication of the region over which surface tension affects the conformation of the thin layer. The film thickness within the boundary layer $\tilde{h}$ is described by

$$\tilde{h}_\tau + [\tilde{h}^3(-\zeta \tilde{h}_{\zeta\zeta\zeta})]_\zeta = 0, \tag{5.13}$$

which is the local form of (5.1) near $\theta = \pi$ for $Bo = 1$ and $\mathscr{A} = 0$. Equation (5.13) is highly nonlinear and must be solved numerically and matched as $\zeta \to \infty$ to the 'outer' solution provided by (5.11). This procedure would provide a uniform approximation for the film thickness over the entire spatial domain for very large Bond number. Instead, in the following section we shall solve the original evolution equation directly for a range of Bond numbers, including the case of very large Bond number.

5.2.3. *Finite Bond number*, $\mathscr{A} = 0$

For finite Bond numbers, the free-surface dynamics are markedly different from those described in the previous section. The film evolution for a layer with very large Bond number ($Bo^{-1} = 0.01$) and no van der Waals forces is shown in figure 5. The film interface has a smooth surface which evolves towards a pendant-drop-like shape over the course of time. The film thins locally and 'necks-down' near the bottom of the substrate. Over time, the drainage slows as the surface curvature of the film at the

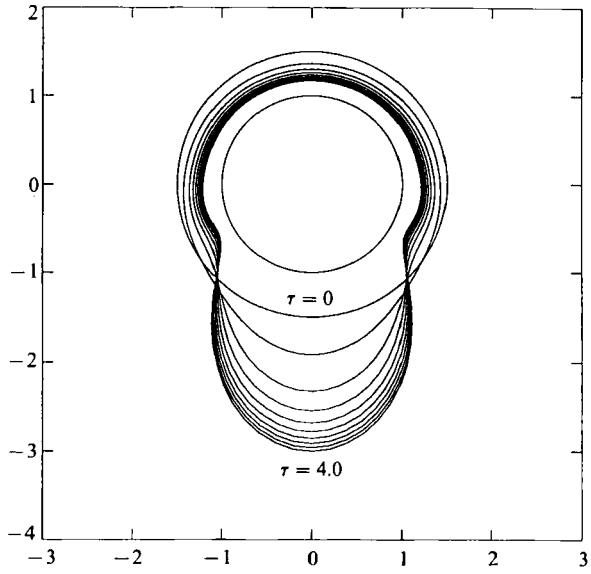

FIGURE 5. Unsteady film flow for the isothermal film with $Bo^{-1} = 0.01, \mathscr{A} = 0$. (The actual film thickness is 2ϵ times that shown.)

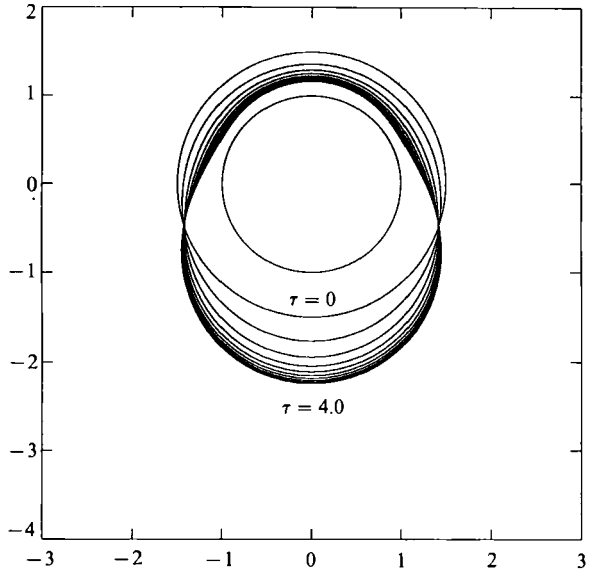

FIGURE 6. Unsteady film flow for the isothermal film with $Bo^{-1} = 0.25, \mathscr{A} = 0$. (The actual film thickness is 2ϵ times that shown.)

substrate base becomes large and the weight of the fluid in the drop becomes balanced by the force of surface tension.

The interfacial dynamics for a smaller Bond number ($Bo^{-1} = 0.25$) are illustrated in figure 6. In this case, the larger surface-tension-to-gravity ratio causes the film to assume a more circular cross-section than in the preceding case. This circular interface is shifted downward owing to gravity and becomes deformed to accommodate the substrate, causing the film to thin locally at two spots in the upper hemicircle of the substrate.

Figure 7 illustrates the dynamic interface position at a fixed time for various Bond

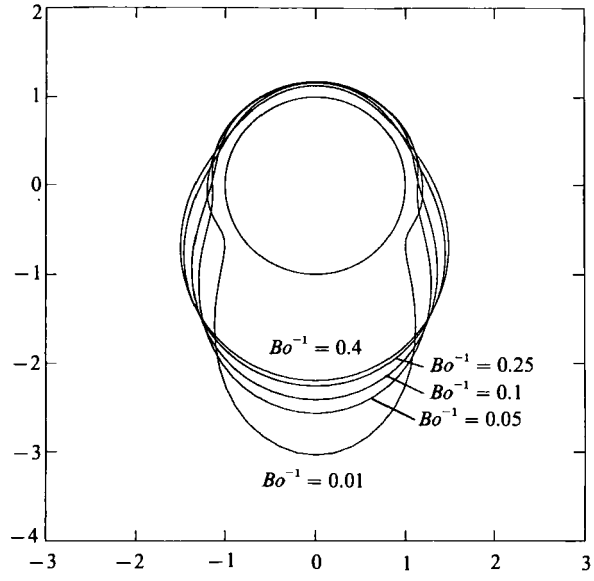

FIGURE 7. Dynamic isothermal film profiles for various values of the Bond number at $\tau = 4.0$. (The actual film thickness is 2ϵ times that shown.)

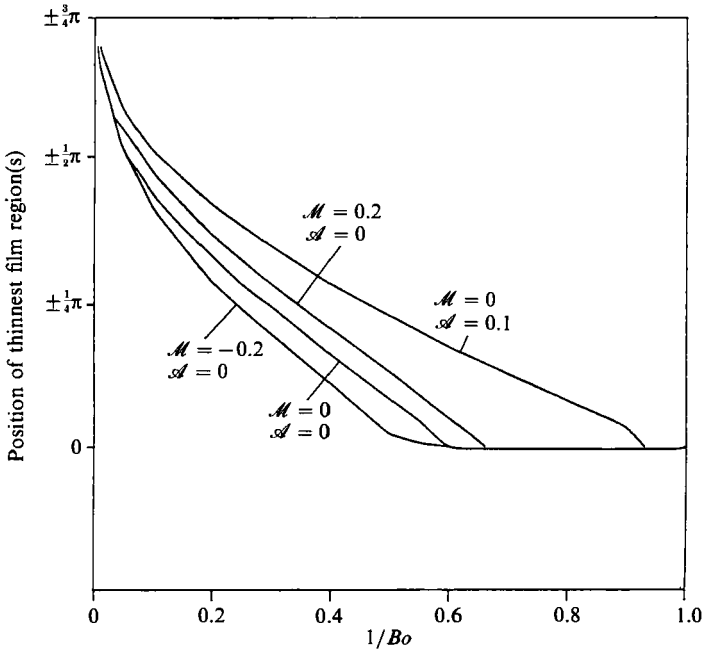

FIGURE 8. Location of local areas of film thinning as a function of the Bond number. Results based on the solution of the full evolution equation to a fixed time, $\tau = 4$.

numbers. Notice that as the Bond number is decreased, the location of the thin regions moves farther and farther towards the top of the substrate ($\theta = 0$). Ultimately, as the Bond number is decreased further, the two thin regions coalesce into a single region at $\theta = 0$. The azimuthal location of the locally-thin film regions as a function of the Bond number is shown in figure 8. For very large Bond numbers ($Bo^{-1} \to 0$) as well as small Bond numbers ($Bo^{-1} > 0.6$), a single spot of film thinning

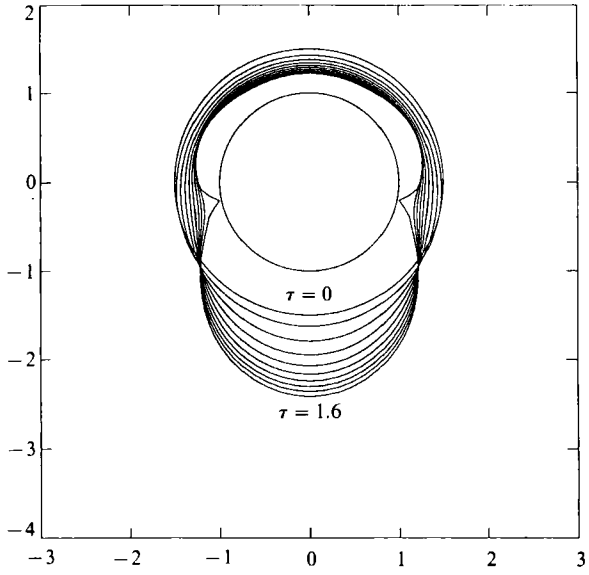

FIGURE 9. Unsteady film flow and rupture for the isothermal film with $Bo^{-1} = 0.05, \mathscr{A} = 0.1$. (The actual film thickness is 2ϵ times that shown.)

Conditions	a	b	Range, Bo^{-1}
$\mathscr{M} = 0, \mathscr{A} = 0$	1.7	3.0	0.05–0.6
$\mathscr{M} = 0, \mathscr{A} = 0.1$	1.7	2.0	0.1–0.6
$\mathscr{M} = 0.2, \mathscr{A} = 0$	1.8	3.0	0.05–0.7
$\mathscr{M} = -0.2, \mathscr{A} = 0$	1.6	3.0	0.1–0.5

TABLE 2. Relationship between azimuthal angle for thinnest film region, θ_m, and the Bond number, $\theta_m = a - b\,Bo^{-1}$

is present, located at the top of the cylinder. When the fluid Bond number is in the range $0 < Bo^{-1} < 0.6$, two locally-thin spots are present, and the azimuthal location of the thin regions decreases monotonically with increasing Bo^{-1}. Over the range $0.05 < Bo^{-1} < 0.6$, the relationship between the azimuthal position of minimum film thickness θ_m and the Bond number can be represented well by the linear equation

$$\theta_m = a - b\,Bo^{-1}, \tag{5.14}$$

where $a = 1.7$ and $b = 3.0$ (see table 2). For $Bo^{-1} \to \infty$, surface tension prevents flow completely and the film retains its initial configuration ($h \equiv 1$), and thus there are no locally-thin regions.

Although derived on the basis of small Bond number, it is interesting to note that in the limit of large Bond number, (5.7) is consistent with (5.14), with $a = \frac{1}{2}\pi$ and $b = 12\tilde{t}/(-1 + e^{-12\tilde{t}} + 12\tilde{t})$.

5.2.4. *Finite Bond number, $\mathscr{A} > 0$*

For very thin liquid films (< 100 nm), intermolecular forces can causc rupture of the layer at locally-thin regions (Ruckenstein & Jain 1974). As figure 9 demonstrates, the film first develops thin spots (as described in §5.2.3) which eventually become spots of film rupture (namely, points at which $h \to 0$). This rupture occurs because

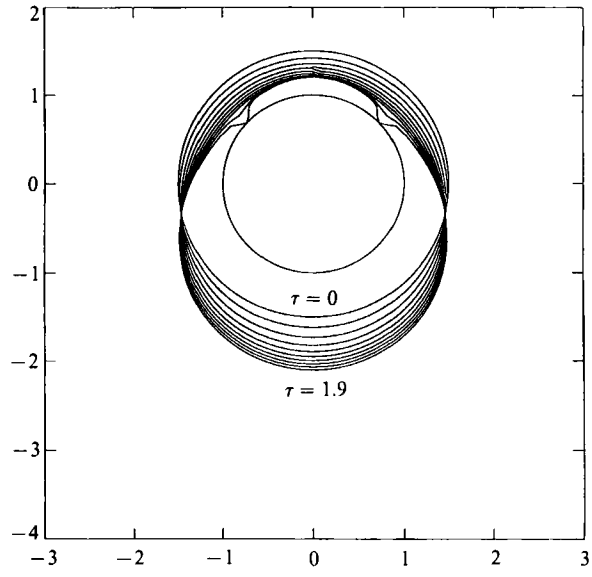

FIGURE 10. Unsteady film flow and rupture for the isothermal film with $Bo^{-1} = 0.5, \mathscr{A} = 0.1$. (The actual film thickness is 2ϵ times that shown.)

intermolecular forces produce a negative disjoining pressure which acts on regions of the film that are thinner than surrounding regions. These destabilizing forces ($\propto 1/h^3$) accelerate the film interface towards the substrate as the film becomes thinner and thinner.

The rupture process at a smaller value of the Bond number is shown in figure 10. As compared to the previous case, the points of film rupture have moved towards the north pole of the cylinder, for the same reasons as outlined previously. In addition, the rupture time is increased owing to the slower film drainage, which is associated with a smaller Bond number. As in the case of $\mathscr{A} = 0$, the azimuthal position of the locally-thin regions is well described over a large range of Bond numbers by (5.14) (See table 2.)

Figure 8 exhibits the fact that the linear portion of the curve for $\mathscr{A} = 0.1$ has a slope which is less than that portion of the curve for $\mathscr{A} = 0$; intermolecular forces destabilize the film at early times even for small Bond numbers. Hence, in the presence of intermolecular forces, there may be two points of film rupture even for small Bond numbers.

6. Results – heated cylinder

When the cylinder is heated, thermocapillary forces generate a flow which augments that due to gravity. As the film thins on the upper surface of the cylinder owing to gravity, there is an increase in temperature in this region and a decrease in surface tension, inducing a flow towards the thicker, higher-surface-tension region at the bottom of the cylinder.

In the absence of intermolecular forces, the appropriate evolution equation describing the interfacial location for a thin liquid film on a heated horizontal cylinder is

$$h_\tau + \left\{ h^3[\sin\theta + Bo^{-1}(h_\theta + h_{\theta\theta\theta})] + B\mathscr{M}\frac{h^2 h_\theta}{(1+Bh)^2} \right\}_\theta = 0. \tag{6.1}$$

6.1. *Steady states*

The presence of thermocapillarity for the heated cylinder enhances drainage from the substrate. Finite surface tension is insufficient to balance the flow and no steady state is possible for the film unless $Bo = 0$, and hence $h(\theta) \equiv 1$.

6.2. *Unsteady flow*

6.2.1. *Small Bond number – early-time dynamics*

As in §5.2.1, when the Bond number is small and van der Waals forces are negligible, we may elucidate the early-time film dynamics. In this case, (6.1) may be solved and the interfacial position given by

$$h \sim 1 + Bo\, F_1(\tilde{t}) \cos\theta + Bo^2 F_2(\tilde{t}) \cos(2\theta), \tag{6.2a}$$

where

$$F_1(\tilde{t}) = \mathscr{R}^{-1}(1 - \mathrm{e}^{\mathscr{R}\tilde{t}}), \tag{6.2b}$$

$$F_2(\tilde{t}) = a_0 + a_1 \mathrm{e}^{\mathscr{R}\tilde{t}} + a_2 \mathrm{e}^{2\mathscr{R}\tilde{t}} + a_3 \mathrm{e}^{4(\mathscr{R}-3)\tilde{t}}, \tag{6.2c}$$

with

$$a_0 = \frac{-(1+B)(1+3B)}{4\mathscr{R}[3+6B+4B^2-\mathscr{R}(1+B)^2]}, \tag{6.2d}$$

$$a_1 = \frac{(1+B)(-1+3B)}{3\mathscr{R}[4+8B+4B^2-\mathscr{R}(1+B)^2]}, \tag{6.2e}$$

$$a_2 = \frac{(1+B)}{\mathscr{R}[6+12B+6B^2-\mathscr{R}(1+B)^2]}, \tag{6.2f}$$

$$a_3 = \frac{(1+B)^3[18+54B+54B^2+18B^3-5\mathscr{R}(1+B)^2-3B\mathscr{R}(1+B)^2]}{12[3+6B+3B^2-\mathscr{R}(1+B)^2][4+8B+4B^2-\mathscr{R}(1+B)^2][6+12B+6B^2-\mathscr{R}(1+B)^2]}, \tag{6.2g}$$

and we have defined a new parameter $\mathscr{R}$,

$$\mathscr{R} = \frac{3CB}{2\epsilon^2(1+B)^2}. \tag{6.3}$$

The value $\mathscr{R} = 0$ denotes an isothermal film, while negative values indicate a cooled film (see §7.2.1).

Figure 11 illustrates the $O(Bo)$ correction to the heated (cooled) film profile at a fixed time for various values of $\mathscr{R}$. As the figure displays, an increase in the film drainage owing to increasing thermocapillarity (increasing $\mathscr{R}$), pushes the interface farther and farther away from the initial conformation, $F_1(0)\cos\theta \equiv 0$.

Analogous to the result obtained in §5.2.1, the $O(Bo^2)$ term in (6.2) suggests the possibility of local minima for the film. The location of these minima is then given by

$$\theta_{\mathrm{m}} = \cos^{-1}\left[\frac{-F_1(\tilde{t})\,Bo^{-1}}{4F_2(\tilde{t})}\right]. \tag{6.4}$$

It is instructive to compare the results from (6.4) relating the location of locally-thin regions for the film with those based on a numerical solution of the full evolution equation as illustrated in figure 8. Although derived on the basis of small Bond

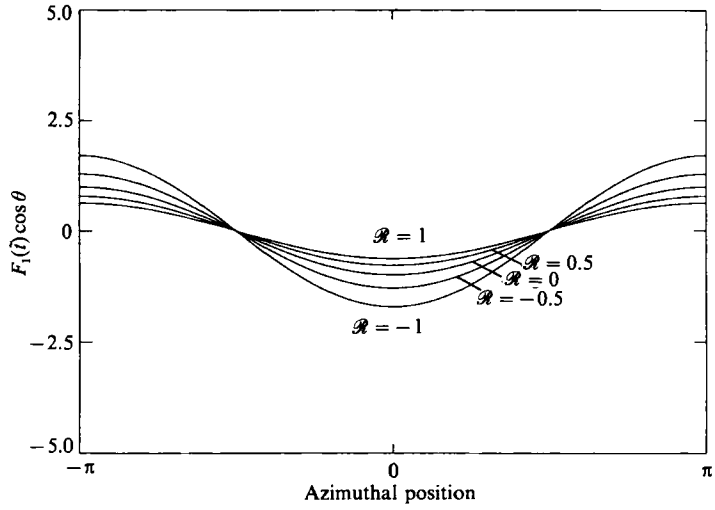

FIGURE 11. Small-Bond-number correction to the thickness profiles for the heated and cooled film at $\tilde{t} = 1$ ($B = 1$).

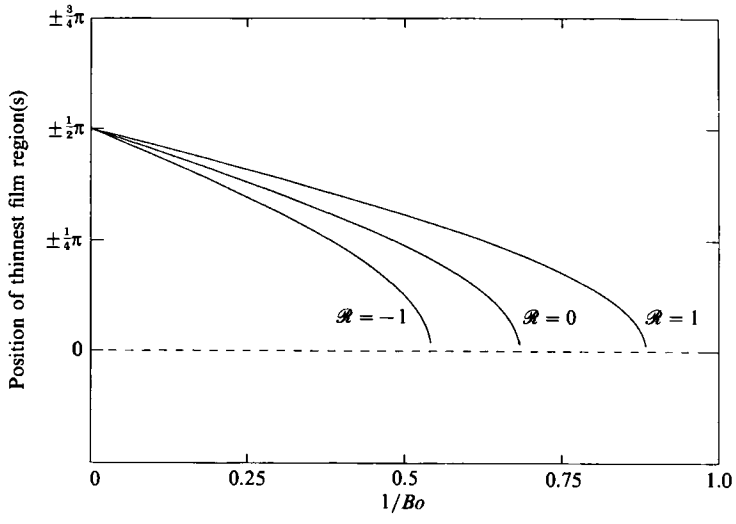

FIGURE 12. Location of local areas of film thinning as a function of the Bond number. Results based on the small-Bond-number analysis at a fixed time, $\tilde{t} = 1$.

number, we note in figure 12 that the theory for small Bond number predicts similar qualitative behaviour and the same trend with regard to thermocapillary effects described in §6.2.2 and illustrated in figure 8.

6.2.2. *Unit-order Bond number*

The forces due to thermocapillarity augment gravity so that the flow at a given time is greater for the heated film than for the isothermal film. Figure 13 shows a 'snapshot' of the evolving film for various values of the effective Marangoni number at a fixed Bond number. (Negative values of $\mathscr{M}$ denote a cooled film. See §7.2.2.) At a given time in the film evolution, increasing the effect of thermocapillarity (increasing $\mathscr{M}$) increases the flow in the film and pushes the interface farther away from the initial configuration.

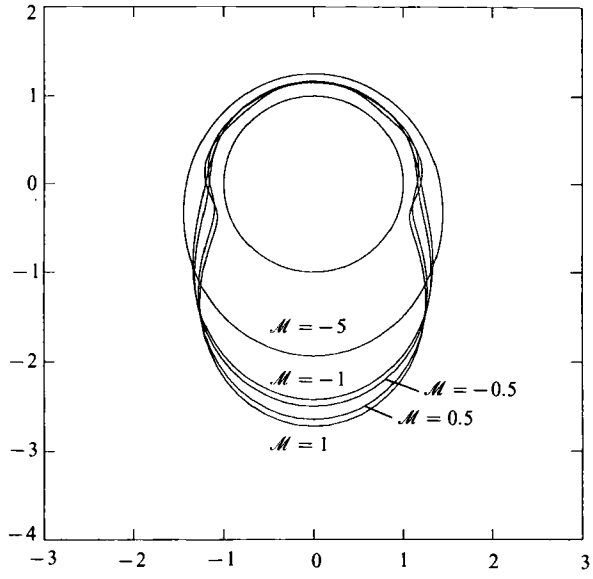

FIGURE 13. Dynamic heated and cooled film profiles for various values of $\mathcal{M}$ at $\tau = 4.0$ ($B = 1$). (The actual film thickness is 2ϵ times that shown.)

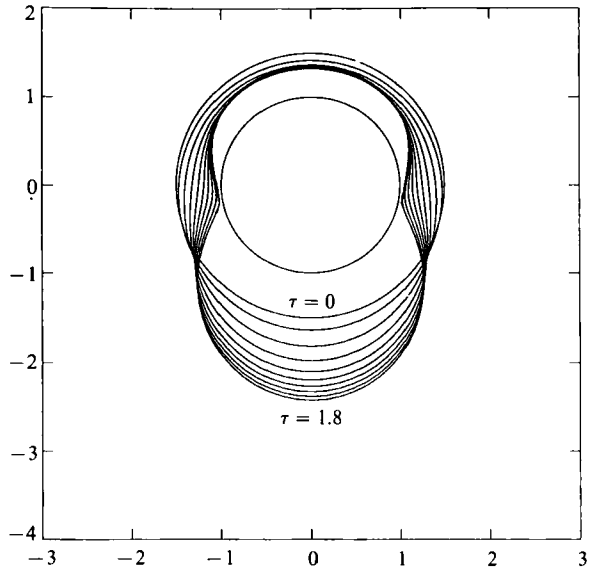

FIGURE 14. Unsteady film flow for the heated film with $Bo^{-1} = 0.2, \mathcal{M} = 3, B = 1$. (The actual film thickness is 2ϵ times that shown.)

Even when intermolecular forces are absent, the film may approach zero thickness owing to thermocapillarity in conjunction with fluid drainage. As suggested by figure 14, regions of the film which are thin owing to the interaction of surface tension and gravity (§5.2) become thinner as fluid is drawn towards the thicker, lower-temperature regions. This process continues until fluid becomes depleted locally and the film nears rupture ($h \to 0$) at the azimuthal location designated in figure 8. Over the range $0.05 < Bo^{-1} < 0.7$, (5.14) (with $a = 1.8$ and $b = 3.0$) represents the location of the locally-thin regions well. Relative to the isothermal result, thermocapillary

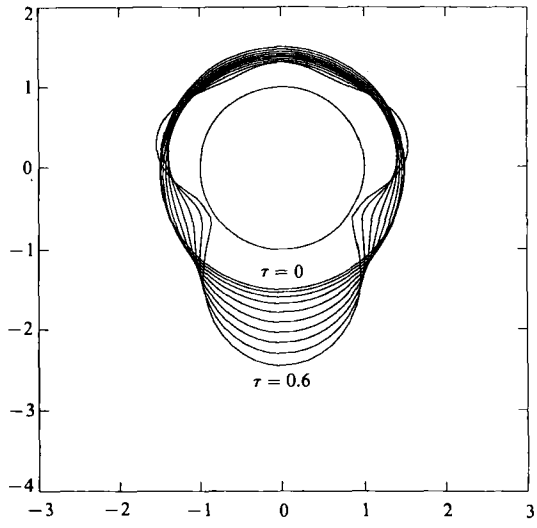

FIGURE 15. Unsteady film flow for the heated film with $Bo^{-1} = 0.1, \mathscr{M} = 5, B = 1$. (The actual film thickness is 2ϵ times that shown.)

forces cause the film to thin at a location which is farther from the top of the cylinder, for a given Bond number; thermocapillary forces 'pull' fluid towards the thicker, cooler film region at the bottom of the cylinder.

If the Marangoni number is increased over that just described, thermocapillary forces are accentuated, and deviations from the mean film thickness, both positive and negative, become more and more exaggerated over time. The peculiar clover-leaf-like shape illustrated in figure 15 is the result of the evolution of the film under these circumstances. It is apparent, then, that a wide variety of interfacial behaviour is possible for a film on a heated horizontal cylinder simply by varying the physical properties of the fluid ($Bo, \mathscr{M}$).

7. Results – cooled cylinder

For a cooled cylinder, thermocapillary forces help to restrain film drainage: as the film thins at the top of the cylinder owing to gravity, the low temperature leads to a large effective surface tension in this region which draws fluid up from the thicker-film regions. To analyse this flow, it is useful to rescale the temperature based on the reference temperature at the substrate surface and then proceed as in §4. Specifically, the temperature difference, $T-T_0$ is scaled on its maximum difference $\Delta T = T_\infty - T_0$, The scaled thermal-flux condition at leading-order becomes

$$T_{0\xi} + B(T_0 + 1) = 0. \tag{7.1}$$

The temperature distribution is found by solving (4.5) subject to conditions (7.1) and (4.7*c*),

$$T_0 = \frac{B\xi}{1+Bh}. \tag{7.2}$$

The free-surface temperature is then

$$T_0 = \frac{Bh}{1+Bh}. \tag{7.3}$$

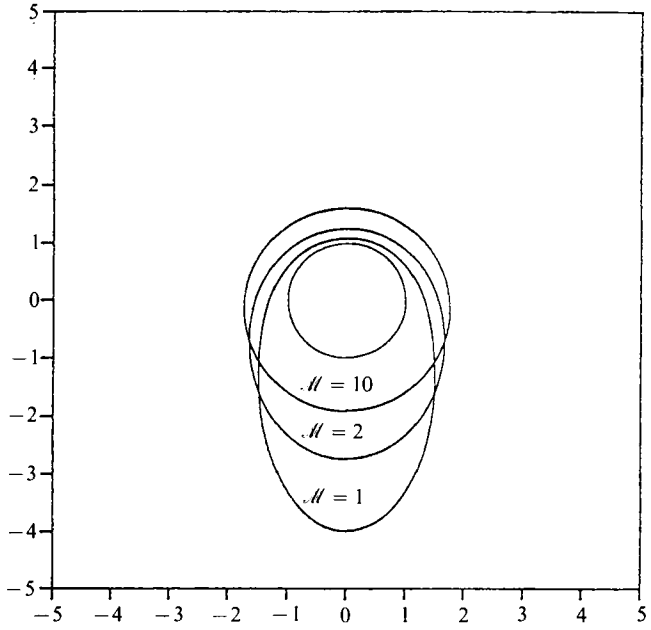

FIGURE 16. Steady-state profiles for the cooled film with unit-order Biot number ($B = 1$). (The actual film thickness is $\frac{4}{3}\epsilon$ times that shown.)

In the adiabatic limit, the free-surface temperature $T_0(h) = 0$, whereas in the surface equilibrium case ($B \to \infty$), the free-surface temperature $T_0(h) = 1$. The evolution equation for the cooled cylinder when van der Waals forces are negligible is identical to that derived for the heated film [equation (6.1)] with $\mathcal{M}$ replaced by $-\mathcal{M}$.

7.1. *Steady states*

For the cooled cylinder, a variety of steady-state profiles may exist. The specific liquid properties and thermal conditions at the liquid/gas interface determine the resulting shape of the fluid interface. The equation

$$\left\{h^3[\sin\theta + Bo^{-1}(h_\theta + h_{\theta\theta\theta})] - B\mathcal{M}\frac{h^2 h_\theta}{(1+Bh)^2}\right\}_\theta = 0 \tag{7.4}$$

governs the steady-state configuration for a film on a cooled cylinder.

7.1.1. *Unit-order Biot number*

For very large Bond number, the form of (7.4) which balances gravity and thermocapillarity is

$$\left[h^3 \sin\theta - B\mathcal{M}\frac{h^2 h_\theta}{(1+Bh)^2}\right]_\theta = 0. \tag{7.5}$$

Equation (7.5) is solved subject to the symmetry boundary conditions to give an implicit solution for the film thickness,

$$B\mathcal{M}\left[\frac{1}{1+Bh} + \ln\left(\frac{h}{1+Bh}\right)\right] + \cos\theta + \gamma = 0, \tag{7.6}$$

where γ is determined from the mass conservation constraint. The steady-state free-surface positions described by (7.6) are shown in figure 16. When the effective Marangoni number is increased, the film interface is deformed less and less from the

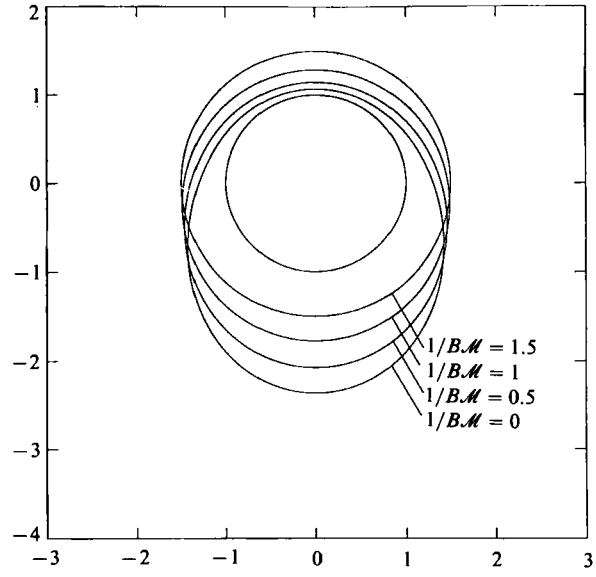

FIGURE 17. Steady-state profiles for the cooled film with small Biot number. (The actual film thickness is 2ϵ times that shown.)

initial shape, as thermocapillarity counteracts gravity increasingly. The interface retains its initial conformation for large $\mathcal{M}$ as the gravity-driven flow downward is inhibited completely.

7.1.2. *Small Biot number*

A very small Biot number implies that the temperature at the free surface is close to that at the (cooled) cylinder surface. This leads to a high effective surface tension and a nearly circular film cross-section. For small Biot numbers, (7.4) may be written as

$$\{h^3[\sin\theta + Bo^{-1}(h_\theta + h_{\theta\theta\theta})] - B\mathcal{M}h^2h_\theta\}_\theta = 0. \tag{7.7}$$

This result describes a balance between gravity and surface tension plus thermocapillarity. It is possible to obtain an explicit solution for the steady-state film thickness from this equation when surface tension is very small relative to gravity. The solution of (7.7) subject to (4.8) and (4.9) is given by

$$h \sim \frac{1}{I_0(1/B\mathcal{M})}\exp\left(-\frac{1}{B\mathcal{M}}\cos\theta\right) + Bo^{-1}\Lambda(\theta), \tag{7.8a}$$

where

$$\Lambda(\theta) = \frac{(B\mathcal{M})^2 + B\mathcal{M}\cos\theta + \sin^2\theta}{(B\mathcal{M})^3 I_0(1/B\mathcal{M})^2}\exp\left(-\frac{2}{B\mathcal{M}}\cos\theta\right) + \frac{I_1(2/B\mathcal{M}) - 2B\mathcal{M}I_0(2/B\mathcal{M})}{2(B\mathcal{M})^2 I_0(1/B\mathcal{M})^3}\exp\left(-\frac{1}{B\mathcal{M}}\cos\theta\right), \tag{7.8b}$$

and I_n is the modified Bessel function of the first kind of order n. Figure 17 details the steady-state film behaviour when the Bond number is large. As shown by this equation, the parameter $1/B\mathcal{M}$ governs the steady-state shape of the fluid interface, indicating that both the Biot number and the effective Marangoni number influence

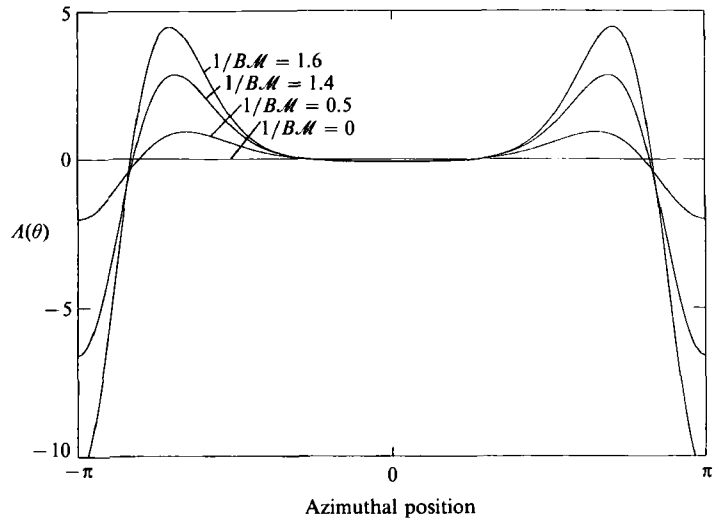

FIGURE 18. Large-Bond-number correction to the steady-state thickness profiles for the cooled film.

the interfacial shape in a similar fashion. Increasing the parameter $1/B\mathcal{M}$ shifts the profile downward, though the shape of the profile remains nearly circular.

The function $\Lambda(\theta)$ corrects the steady-state balance between gravitational and thermocapillary forces for the existence of finite surface tension. As shown in figure 18, the presence of finite Bo^{-1} leads to a local thinning at $\theta = \pi$, in addition to points of local thickening not present in the leading-order behaviour.

7.1.3. *Large Biot number*

Large Biot numbers specify a free surface which is nearly in equilibrium with the environment. In this case, the surface tension, especially at thicker-film regions, is relatively small. Therefore, the film distorts from the initial shape, especially at the base of the substrate. When the Biot number is large, (7.4) takes the form

$$\{h^3[\sin\theta + Bo^{-1}(h_\theta + h_{\theta\theta\theta})] - \mathcal{M}h_\theta/B\}_\theta = 0, \tag{7.9}$$

which, for large Bond numbers, has the solution

$$h \sim \left(\frac{2B}{\mathcal{M}}\cos\theta + \delta_1\right)^{-\frac{1}{2}} + Bo^{-1}\left\{\left[\frac{3B^3}{\mathcal{M}^3}(1+\cos^2\theta) + \frac{5B^2}{\mathcal{M}^2}\delta_1\cos\theta + \frac{B}{\mathcal{M}}\delta_1^2\right]\left(\delta_1 + \frac{2B}{\mathcal{M}}\cos\theta\right)^{-4} + \delta_2\left(\delta_1 + \frac{2B}{\mathcal{M}}\cos\theta\right)^{-\frac{3}{2}}\right\}, \tag{7.10a}$$

where δ_1 is determined as the solution of the equation

$$K\left(\frac{4B/\mathcal{M}}{\delta_1 + 2B/\mathcal{M}}\right)^{\frac{1}{2}} = \tfrac{1}{2}\pi\left(\delta_1 + \frac{2B}{\mathcal{M}}\right)^{\frac{1}{2}}, \tag{7.10b}$$

with

$$K(\alpha) = \int_0^{\frac{1}{2}\pi} \frac{\mathrm{d}\theta}{(1-\alpha^2\sin^2\theta)^{\frac{1}{2}}} \tag{7.10c}$$

the complete elliptic integral of the first kind; δ_2 is determined by the mass conservation constraint. From (7.10), the parameter $B/\mathcal{M}$ controls the steady-state

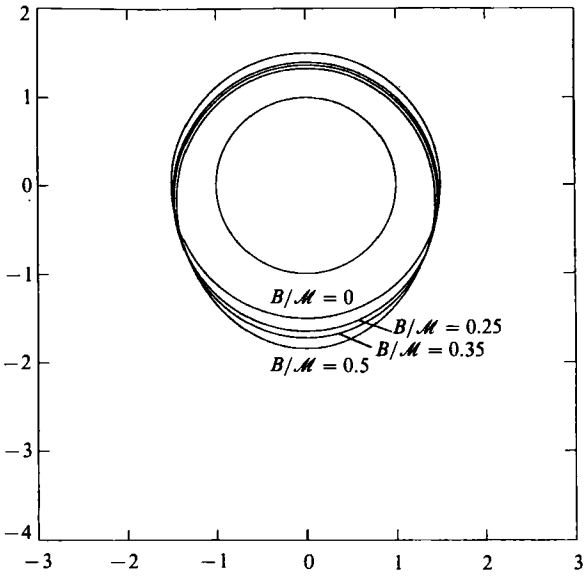

FIGURE 19. Steady-state profiles for the cooled film with large Biot number. (The actual film thickness is 2ϵ times that shown.)

shape of the interface, but unlike the small-Biot-number situation, the Biot number and Marangoni number affect the conformation of the free surface in disparate directions. Figure 19 shows in this case that increasing the parameter $B/\mathscr{M}$ causes the interface to become deformed from its initial state, especially at the thicker-film region at the bottom of the cylinder.

7.2. *Unsteady flow*

7.2.1. *Small Bond number – early-time dynamics*

Like the isothermal film and film on the heated cylinder (§§5.2.1 and 6.2.1), in the limit of small Bond number and vanishing van der Waals forces, the behaviour of the film at early times may be examined using a regular perturbation analysis. In this context, (6.1) is solved and the resulting film thickness is given by (6.2) with $\mathscr{R}$ replaced by $-\mathscr{R}$.

7.2.2. *Unit-order Bond number*

When the flow is unsteady, the role of thermocapillary forces is to retard the gravity-driven drainage from the cylinder. Figure 13 shows the film profile at $\tau = 4.0$ for various values of $-\mathscr{M}$. In contrast to the heated cylinder, as $|\mathscr{M}|$ is increased, drainage from the film is reduced, and the interface deforms less and less from the initial configuration. For large enough $|\mathscr{M}|$, therefore, thermocapillarity overcomes gravity and the film evolves to a steady-state or retains its uniform initial shape. Over the range $0.1 < Bo^{-1} < 0.5$, (5.14) (with $a = 1.6$ and $b = 3.0$) represents the location of the locally-thin regions well. Relative to the isothermal result, for the cooled cylinder, thermocapillary forces cause the film to thin at a location which is closer to the top of the cylinder, for a given Bond number; thermocapillary forces pull fluid towards the thinner, cooler film region at the top of the cylinder.

8. Linear stability of the basic state

The governing two-dimensional equations (2.1)–(2.16) are readily generalized to include variations in the axial direction, denoted by z (scaled by the cylinder radius, R). In a similar manner to that detailed earlier, we obtain the two-dimensional analogue of (4.17):

$$h_\tau + (h^3 \sin\theta)_\theta + Bo^{-1}\nabla\cdot[h^3\nabla(\nabla^2 h + h)] + \nabla\cdot[(B\mathscr{M}h^2(1+Bh)^{-2} + \mathscr{A}h^{-1})\nabla h] = 0, \quad (8.1)$$

where $\nabla = (\partial/\partial\theta, \partial/\partial z)$ is the two-dimensional surface-gradient operator.

Throughout the analysis we have neglected axial variations to the film. We proceed to examine this restriction by investigating the consequence of small axial disturbances to the basic state of the thin layer. In the general case, it is not possible to obtain an analytical solution for the film basic state. We shall, therefore, consider the stability of the film in two limiting cases for which the basic-state behaviour of the layer has been determined analytically: (i) the unsteady isothermal film in the limit of small Bond number (§5.1.1), and (ii) the steady cooled film in the limit of large Bond number (§7.1.2).

Case (i). Unsteady isothermal film

In this case we shall investigate the special case of axial disturbances imposed on the small Bond number basic state derived earlier (equation (5.6)); specifically,

$$\bar{h}(\theta,\tau) = 1 - Bo\,\tilde{t}\cos\theta = 1 - \tau\cos\theta, \quad (8.2)$$

where the overbar denotes the basic state. We employ linear theory and perturb this state by a small amount h'. We therefore write

$$h(\theta,z,\tau) = \bar{h}(\theta,\tau) + h'(\theta,z,\tau), \quad (8.3)$$

and assume normal modes in the disturbance quantity h' of the form

$$h'(\theta,z,\tau) = H(\theta,\tau)\,e^{ikz}, \quad (8.4)$$

where k is the disturbance wavenumber. Substituting (8.4) into (8.3), (8.3) into (8.1), and linearizing in the Bond number results in a partial differential equation for the normal-mode amplitude H,

$$H_\tau + Bo^{-1}[H_{\theta\theta\theta} + (1-2k^2)H_{\theta\theta} - k^2(1-k^2)H] = 0. \quad (8.5)$$

The solution of (8.5), consistent with the symmetry conditions, may be written as

$$H(\theta,\tau) = \sum_{n=0}^{\infty} c_n \exp(\omega_n \tau)\cos(n\theta) = \sum_{n=0}^{\infty} c_n \exp(\Omega_n \tilde{t})\cos(n\theta), \quad (8.6a)$$

where

$$c_n = \frac{2}{\pi}\int_0^{\pi} H(\zeta)\cos(n\zeta)\,d\zeta, \quad (8.6b)$$

and the disturbance growth rate $\omega_n(\Omega_n)$ is

$$Bo\,\omega_n = \Omega_n = -(k^2+n^2)(k^2+n^2-1). \quad (8.6c)$$

The maximum growth rate occurs for $n = 0$,

$$Bo\,\omega_0 = \Omega_0 = k^2(1-k^2), \quad (8.7)$$

corresponding to the axisymmetric disturbance mode; all other modes are either neutrally stable or stable for all k.

From (8.7) we note that the layer is stable for large wavenumbers ($k > 1$) and is unstable for wavenumbers in the range $0 < k < 1$. The wavenumber k^* relating to the maximum growth rate ω^* is determined to be

$$k^* = \frac{1}{\sqrt{2}}, \tag{8.8}$$

and is identical to that computed by Goren (1962) for a thin annulus of fluid on a wire in the absence of gravity; the corresponding maximum growth rate is then

$$Bo\,\omega^* = \Omega^* = \tfrac{1}{4}. \tag{8.9}$$

This analysis reveals that a small Bond number does not destabilize the film relative to the film with zero Bond number. We also see that axial variations to the layer are unimportant as long as $\tau \ll 4Bo\,(\tilde{t} \ll 4)$, but will become significant thereafter as the film continues to drain. For large Bond number, drainage from the substrate is relatively rapid, and hence the timescale over which the film resides on the cylinder surface is relatively short. We therefore expect the dynamics of the layer to be less affected by axial variations than those for the layer with small Bond number. This trend is expected for the heated film as well, since thermocapillarity augments the gravity-driven flow off the substrate; we expect the unsteady cooled film to be more affected by axial variations for the opposite reason.

Case (ii). Steady cooled film

Here we shall examine axial disturbances imposed on the known steady basic state for a film on a cooled cylinder in the limit of small Biot number and very large Bond number (equation (7.8*a*)), namely,

$$\bar{h}(\theta) = \frac{1}{I_0(1/B\mathscr{M})}\exp\left(-\frac{1}{B\mathscr{M}}\cos\theta\right). \tag{8.10}$$

Similar to the previous case, we perturb the basic state by a small amount,

$$h(\theta, z, \tau) = \bar{h}(\theta) + h'(\theta, z, \tau), \tag{8.11}$$

and assume normal modes in the disturbance quantity of the form

$$h'(\theta, z, \tau) = H(\theta)\,\mathrm{e}^{\mathrm{i}kz+\omega\tau}. \tag{8.12}$$

Substituting (8.12) into (8.11), (8.11) into (8.1), and linearizing in primed quantities results in an ordinary differential equation for the normal-mode amplitude H,

$$H_{\theta\theta} + \frac{1}{B\mathscr{M}}\sin\theta H_\theta - \frac{1}{(B\mathscr{M})^2}\psi(\theta)H = 0, \tag{8.13a}$$

where

$$\psi(\theta) = 2\sin^2\theta + B\mathscr{M}\cos\theta + (B\mathscr{M})^2k^2 + B\mathscr{M}\exp\left(\frac{2}{B\mathscr{M}}\cos\theta\right)\left[I_0\left(\frac{1}{B\mathscr{M}}\right)\right]^2\omega. \tag{8.13b}$$

Taking into account symmetry conditions, we write the normal-mode amplitude as a Fourier cosine series,

$$H(\theta) = \sum_{n=0}^{\infty} b_n \cos(n\theta), \tag{8.14}$$

leading to the equation $$\sum_{n=0}^{\infty} b_n \Gamma(\theta, n) = 0, \tag{8.15a}$$

where

$$\Gamma(\theta, n) = \left\{ n^2 + k^2 + \frac{2}{(B\mathcal{M})^2}\sin^2\theta + \frac{1}{B\mathcal{M}}\cos\theta + \frac{1}{B\mathcal{M}}\exp\left(\frac{2}{B\mathcal{M}}\cos\theta\right)\left[I_0\left(\frac{1}{B\mathcal{M}}\right)\right]^2 w \right\}\cos n\theta + \frac{n}{B\mathcal{M}}\sin\theta\sin(n\theta). \tag{8.15b}$$

The stability characteristics of the liquid layer are determined from (8.15). This infinite series is truncated to p-modes; corresponding to each mode is an orthogonality condition. Each of the orthogonality conditions is applied in turn to the truncated Fourier expansion to yield p-simultaneous equations for the unknowns $b_n\,[n = 0, \ldots, p-1]$. To ensure a non-trivial solution for H, we require the determinant of the coefficient matrix of b_n to vanish, leading to a dispersion relationship between the disturbance growth rate and wavenumber. Rootfinding is then used to locate the wavenumber k^* corresponding to the maximum growth rate ω^*.

For $p = 1$, the dispersion relationship is found to be

$$\omega = -\frac{1 + (B\mathcal{M})^2 k^2}{B\mathcal{M}\,[I_0(1/B\mathcal{M})]^2 I_0(2/B\mathcal{M})}, \tag{8.16}$$

and hence $$k^* = 0, \quad \omega^* = -\frac{1}{B\mathcal{M}\,[I_0(1/B\mathcal{M})]^2 I_0(2/B\mathcal{M})}. \tag{8.17a, b}$$

The analysis of larger numbers of modes confirms that $k^* = 0$ and $\omega^* \leqslant 0$ for all $B\mathcal{M}$. These results suggest that the film will be linearly stable for any solution where thermocapillary forces are large enough to counteract gravity and to maintain a steady-state for the thin layer. We observe that although the stability analysis presented is valid only for small disturbances about the steady basic state (7.8a), it nonetheless confirms that ignoring axial variations to the thin film is appropriate in this case.

9. Conclusions

We investigate the drainage of a thin liquid film on the surface of a heated or cooled horizontal cylinder. We examine the role of gravity, surface tension, thermocapillarity, and van der Waals forces on the dynamics of the film, and explore the possibility of steady states for the film under a variety of thermal conditions.

For an isothermal layer, we find that a steady-state configuration for the layer is possible only for a zero Bond number. For non-zero Bond numbers, the film is unsteady and we discover that areas of local thinning can develop as the film drains. We quantify the azimuthal location of the locally-thin regions as a function of the Bond number, and find that these regions move towards the top of the cylinder as the Bond number is decreased, until, for very small Bond numbers, two regions coalesce into a single region at the top of the cylinder. For very thin films for which destabilizing intermolecular forces may be appreciable, we observe that these locally-thin spots can become spots of film rupture.

We discover that a wide variety of interfacial behaviour is possible for a film on

a heated horizontal cylinder. Thermocapillary forces augment the effect of gravity and increase the rate of drainage off the cylinder. When the Marangoni number is sufficiently large, the film thickness can become very small locally, and in the presence of intermolecular forces, rupture of the film interface occurs. Simply by varying the physical properties of the fluid ($Bo, \mathcal{M}$), it is possible to prevent (promote) film rupture depending upon the application of interest.

If the cylinder is cooled, thermocapillary effects oppose drainage from the surface and we determine that it is possible to restrain the flow for even large Bond numbers. We examine the role of both the free-surface thermal condition (through the Biot number) and the fluid properties (through the Bond and Marangoni numbers) on the steady and unsteady interfacial shapes for the film.

Finally, we use linear theory to determine the stability of the thin layer to small axial disturbances. We consider the stability of the film in two limiting cases: (i) the unsteady isothermal film in the limit of small Bond number, and (ii) the steady cooled film in the limit of large Bond number. In the first case, we find that axial variations to the layer are unimportant at early times, but will become considerable later in the evolution of the film. In the second case, we discover that the film will be linearly stable for any solution where thermocapillary forces are large enough to maintain a steady-state for the thin layer.

The authors wish to thank Professor S. H. Davis and one of the reviewers for their helpful advice and suggestions. This work was supported in part by the US Department of Energy, Division of Basic Energy Science, through Grant no. DE FG02-86ER 13641.

REFERENCES

ATHERTON, R. W. & HOMSY, G. M. 1976 On the derivation of evolution equations for interfacial waves. *Chem. Engng Commun.* **2**, 57.

BANKOFF, S. G. 1971 Stability of liquid flow down a heated inclined plane. *Intl J. Heat Mass Transfer* **14**, 377.

BENNEY, D. J. 1966 Long waves on liquid films. *J. Maths & Phys.* **45**, 150.

BURELBACH, J. B., BANKOFF, S. G. & DAVIS, S. H. 1988 Nonlinear stability of evaporating/condensing liquid films. *J. Fluid Mech.* **195**, 463.

BURELBACH, J. B., BANKOFF, S. G. & DAVIS, S. H. 1990 Steady thermocapillary flows of thin liquid layers. I. Experiment. *Phys. Fluids* A **2**, 322.

DAVIS, S. H. 1983 Rupture of thin liquid films. In *Waves on Fluid Interfaces* (ed. R. E. Meyer), *Proc. Symp. Math. Res. Center, Univ. of Wisc.* pp. 291–302. Academic.

DERYAGIN, B. V. & KUSAKOV, M. M. 1937 *Izv. Akad. Nauk SSSR Khim.* **5**, 1119.

GOREN, S. L. 1962 The instability of an annular thread of fluid. *J. Fluid Mech.* **12**, 309.

JOHNSON, R. E. 1988 Steady-state coating flows inside a rotating horizontal cylinder. *J. Fluid Mech.* **190**, 321.

LIFSHITZ, E. M. 1956 The theory of molecular attractive forces between solids. *Sov. Phys., J. Exp. Theor. Phys.* **2**, 73.

LIN, S. P. 1975 Stability of liquid flow down a heated inclined plane. *Letters in Heat and Mass Transfer*, vol. 2, pp. 361–370. Pergamon.

MOFFATT, K. 1977 Behavior of viscous film on the outer surface of a rotating cylinder. *J. Méc.* **16**, 651.

PITTS, E. 1973 The stability of pendant liquid drops. Part 1. Drops formed in a narrow gap. *J. Fluid Mech.* **59**, 753.

PREZIOSI, L. & JOSEPH, D. 1988 The run-off condition for coating and rimming flow. *J. Fluid Mech.* **187**, 99.

RAYLEIGH, LORD 1879 On the capillary phenomena of jets. *Proc. R. Soc. Lond.* A **29**, 71.

RUCKENSTEIN, E. & JAIN, R. K. 1974 Spontaneous rupture of thin liquid films. *J. Chem. Soc. Faraday Trans.* II **70**, 132.

SPINDLER, B. 1982 Linear stability of liquid films with interfacial phase change. *Intl J. Heat Mass Transfer* **25**, 161.

TAN, M. J., BANKOFF, S. G. & DAVIS, S. H. 1990 Steady thermocapillary flows of thin liquid layers. II. Theory. *Phys. Fluids* A **2**, 313.

VISSER, J. 1972 On Hamaker constants: A comparison between Hamaker constants and Lifshitz–Van der Waals constants. *Adv. Colloid Interface Sci.* **3**, 331.

WILLIAMS, M. B. & DAVIS, S. H. 1982 Nonlinear theory of film rupture. *J. Colloid Interface Sci.* **90**, 220.

XU, J. J. & DAVIS, S. H. 1985 Instability of capillary jets with thermocapillarity. *J. Fluid Mech.* **161**, 1.